

Realization of near-field linear nano-polarizer by asymmetric nanoaperture and bowtie nanoantenna

Jianxiong Li,¹ Shuqi Chen,^{1,*} Ping Yu,¹ Hua Cheng,¹ Xiaoyang Duan,¹
and Jianguo Tian^{1,2}

¹The Key Laboratory of Weak Light Nonlinear Photonics, Ministry of Education, School of Physics and Teda Applied Physics School, Nankai University, Tianjin 300071, China

²jjtian@nankai.edu.cn

*schen@nankai.edu.cn

Abstract: We present a linear nano-polarizer composed of asymmetric nanoaperture and bowtie nanoantenna, which provides a new way to freely control the polarization azimuth of the translated optical field in the near-field. It can not only generate large localized field enhancement and outstanding spatial confinement, but also maintain the polarization azimuth of linearly polarized optical field excited by arbitrary linearly, circularly or elliptically polarized lights. The response wavelength of the linear nano-polarizer can be easily tuned in a wide range by adjusting the geometrical parameters of asymmetric nanoaperture. This offers a further step in developing integrated optical devices for polarization manipulation.

© 2013 Optical Society of America

OCIS codes: (160.3918) Metamaterials; (240.6680) Surface plasmons; (260.5430) Polarization.

References and links

1. R. A. Shelby, D. R. Smith, and S. Schultz, "Experimental verification of a negative index of refraction," *Science* **292**(5514), 77–79 (2001).
2. N. Yu, P. Genevet, M. A. Kats, F. Aieta, J.-P. Tetienne, F. Capasso, and Z. Gaburro, "Light propagation with phase discontinuities: Generalized laws of reflection and refraction," *Science* **334**(6054), 333–337 (2011).
3. L. Novotny and N. van Hulst, "Antennas for light," *Nat. Photon.* **5**(2), 83–90 (2011).
4. D. Dregely, R. Taubert, J. Dorfmueller, R. Vogelgesang, K. Kern, and H. Giessen, "3D optical Yagi-Uda nanoantenna array," *Nat. Commun.* **2**, 267 (2011).
5. S. Chen, H. Cheng, H. Yang, J. Li, X. Duan, C. Gu, and J. Tian, "Polarization insensitive and omnidirectional broadband near perfect planar metamaterial absorber in the near infrared regime," *Appl. Phys. Lett.* **99**(25), 253104 (2011).
6. N. Liu, M. Mesch, T. Weiss, M. Hentschel, and H. Giessen, "Infrared perfect absorber and its application as plasmonic sensor," *Nano Lett.* **10**(7), 2342–2348 (2010).
7. K. M. Dani, Z. Ku, P. C. Upadhy, R. P. Prasankumar, A. J. Taylor, and S. R. J. Brueck, "Ultrafast nonlinear optical spectroscopy of a dual-band negative index metamaterial all-optical switching device," *Opt. Express* **19**(5), 3973–3983 (2011).
8. D. J. Cho, W. Wu, E. Ponizovskaya, P. Chaturvedi, A. M. Bratkovsky, S.-Y. Wang, X. Zhang, F. Wang, and Y. R. Shen, "Ultrafast modulation of optical metamaterials," *Opt. Express* **17**(20), 17652–17657 (2009).
9. B. Memarzadeh and H. Mosallaei, "Array of planar plasmonic scatterers functioning as light concentrator," *Opt. Lett.* **36**(13), 2569–2571 (2011).
10. J. Han, H. Li, Y. Fan, Z. Wei, C. Wu, Y. Cao, X. Yu, F. Li, and Z. Wang, "An ultrathin twist-structure polarization transformer based on fish-scale metallic wires," *Appl. Phys. Lett.* **98**(15), 151908 (2011).
11. A. Roberts and L. Lin, "Plasmonic quarter-wave plate," *Opt. Lett.* **37**(11), 1820–1822 (2012).

12. B. Helgert, E. Pshenay-Severin, M. Falkner, C. Menzel, C. Rockstuhl, E.-B. Kley, A. Tnnemann, F. Lederer, and T. Pertsch, "Chiral metamaterial composed of three-dimensional plasmonic nanostructures," *Nano Lett.* **11**(10), 4400–4404 (2011).
13. J. N. Anker, W. P. Hall, O. Lyandres, N. C. Shah, J. Zhao, and R. P. Van Duyne, "Biosensing with plasmonic nanosensors," *Nat. Mater.* **7**(6), 442–453 (2008).
14. B. K. Canfield, H. Husu, J. Laukkanen, B. Bai, M. Kuittinen, J. Turunen, and M. Kauranen, "Local field asymmetry drives second-harmonic generation in noncentrosymmetric nanodimers," *Nano Lett.* **7**(5), 1251–1255 (2007).
15. M. Hentschel, T. Utikal, H. Giessen, and M. Lippitz, "Quantitative modeling of the third harmonic emission spectrum of plasmonic nanoantennas," *Nano Lett.* **12**(7), 3778–3782 (2012).
16. D. E. Chang, A. S. Sørensen, P. R. Hemmer, and M. D. Lukin, "Quantum optics with surface plasmons," *Phys. Rev. Lett.* **97**(5), 053002 (2006).
17. N. Engheta, "Circuits with light at nanoscales: Optical nanocircuits inspired by metamaterials," *Science* **317**(5845), 1698–1702 (2007).
18. Y. Fan, J. Han, Z. Wei, C. Wu, Y. Cao, X. Yu, and H. Li, "Subwavelength electromagnetic diode: One-way response of cascading nonlinear meta-atoms," *Appl. Phys. Lett.* **98**(15), 151903 (2011).
19. F. Wang, A. Chakrabarty, F. Minkowski, K. Sun, and Q.-H. Wei, "Polarization conversion with elliptical patch nanoantennas," *Appl. Phys. Lett.* **101**(2), 023101 (2012).
20. P. Biagioni, M. Savoini, J. S. Huang, L. Duo, M. Finazzi, and B. Hecht, "Near-field polarization shaping by a near-resonant plasmonic cross antenna," *Phys. Rev. B* **80**(15), 153409 (2009).
21. E. Ögüt, and K. Şendur, "Circularly and elliptically polarized near-field radiation from nanoscale subwavelength apertures," *Appl. Phys. Lett.* **96**(14), 141104 (2010).
22. P. B. Johnson, and R. W. Christy, "Optical constants of the noble metals," *Phys. Rev. B* **6**(12), 4370–4379 (1972).
23. COMSOL 3.4, Comsol Multiphysics, <http://www.comsol.com>.
24. N. A. Hatab, C.-H. Hsueh, A. L. Gaddis, S. T. Retterer, J.-H. Li, G. Eres, Z. Zhang, and B. Gu, "Free-standing optical gold bowtie nanoantenna with variable gap size for enhanced Raman spectroscopy," *Nano Lett.* **10**(12), 4952–4955 (2010).
25. Z. Zhang, A. Weber-Bargioni, S. W. Wu, S. Dhuey, S. Cabrini, and P. J. Schuck, "Manipulating nanoscale light fields with the asymmetric bowtie nano-colorsorter," *Nano Lett.* **9**(12), 4505–4509 (2009).
26. T. H. Taminiou, F. D. Stefani, F. B. Segerink, and N. F. van Hulst, "Optical antennas direct single-molecule emission," *Nat. Photon.* **2**(4), 234–237 (2008).
27. E. Wu, Y. Chi, B. Wu, K. Xia, Y. Yokota, K. Ueno, H. Misawa, and H. Zeng, "Spatial polarization sensitivity of single Au bowtie nanostructures," *J. Lumin.* **131**(9), 1971–1974 (2011).
28. T. Setälä, A. Shevchenko, M. Kaivola, and A. T. Friberg, "Degree of polarization for optical near fields," *Phys. Rev.* **66**(1), 016615 (2002).
29. T. Funk, A. Deb, S. J. George, H. Wang, and S. P. Cramer, "X-ray magnetic circular dichroism—a high energy probe of magnetic properties," *Coord. Chem. Rev.* **249**(1), 3–30 (2005).

1. Introduction

Metamaterials (MMs) have drawn much attention in recent years due to many fascinating properties [1, 2]. Based on their capabilities, MMs have realized the miniaturization of optical components, such as optical antenna [3, 4], perfect absorber [5, 6], optical switch [7, 8], light concentrator [9], polarization transformer [10] and nano-waveplate [11, 12]. These metallic devices have opened up an access to control and guide light in both the near- and far-fields, which can contribute to a wide range of applications in biosensing [13], nonlinear optics [14, 15], quantum optics [16], and optical circuits [17, 18] to name a few. Recently, there has been an increasing interest in developing materials that can manipulate the polarization state of transmitted or reflected light in the far-field [19]. A quarter-wave plate has been achieved by adjusting the degree of asymmetry [11]. In the near-field, the MMs that can transform and control the local polarization state have also been reported. Paolo Biagioni *et al.* proposed an asymmetric cross antenna, constituted by two perpendicular dipole antennas with common feed gap but different lengths [20]. By tuning the response of each antenna, the cross antenna can transform a linearly polarized propagating wave into circularly polarized localized fields, realizing the behavior of a near-field quarter-wave nano-waveplate. Erdem Ögüt *et al.* also presented that a linearly polarized light can be converted into a circularly or elliptically polarized optical spot by creating and adjusting the asymmetry in the aperture dimensions, as well as adjusting the polarization angle of the incident light [21].

In terms of the capacity of these metallic devices to manipulate light interacting with them, the previous designs usually focused on converting the polarization state of the linearly polarized light in the near- or far-field. However, there is seldom research on manipulating the polarization azimuth of linearly polarized optical field in the near- or far-field. The polarization azimuth in near-field can be considered as the localized electric field polarization. It is well known that polarized photons represent a fundamental probe to study the behavior of electrons in matter at optical frequencies. Thus optical fields with a well-defined electric field polarization are of primary importance in many optics applications, such as in spectroscopy and microscopy. Traditionally, Glan-Taylor polarizer consisting of birefringent materials has been employed to control the polarization azimuth of the transmitted light in the far-field, which allows the transmission of a single linear light polarized along the optical axes of the crystals. It has become an indispensable asset to optical experiments and practical applications. If the function of Glan-Taylor polarizer can be realized in the near- or far-fields through MMs, the miniaturization of linear polarizer will be highly desirable for applications in optical nanocircuitry and integrated plasmonic devices.

In this paper, we present a linear nano-polarizer composed of asymmetric nanoaperture and bowtie nanoantenna, which provides a new way to freely control the polarization azimuth of the translated optical field in the near-field. The linear nano-polarizer can generate large enhancement and outstanding spatial confinement of linearly polarized optical field with a fixed polarization azimuth excited by arbitrary linearly, circularly or elliptically polarized lights. Meanwhile, its response wavelength can also be easily tuned in a wide range by adjusting the geometrical parameters of asymmetric nanoaperture. The translated mechanisms of the linearly polarized optical field are also discussed.

2. Combination of asymmetric nanoaperture and bowtie nanoantenna

The designed near-field linear nano-polarizer composed of asymmetric nanoaperture and bowtie nanoantenna is shown in Fig. 1. The asymmetric nanoaperture consists of two crossed rectangular nanoapertures in a gold film with thickness $h=60$ nm. The lengths of the rectangular nanoapertures are $L_1=230$ nm and $L_2=170$ nm, respectively, and the widths are both 50 nm. The cross angle between two rectangles is equal to 60° , which is bisected by x -axis. A 20-nm-thick bowtie nanoantenna is located at the bottom of the asymmetric nanoaperture. The symmetry axis of the bowtie nanoantenna along the perpendicular bisector of the triangle is

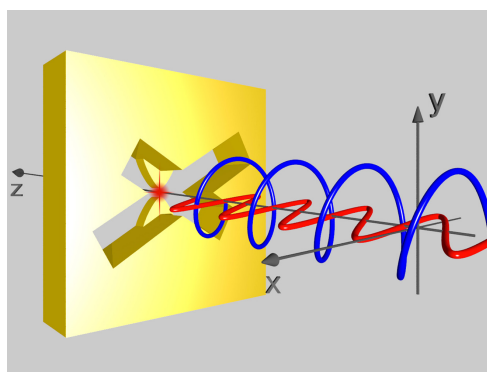


Fig. 1. The designed linear nano-polarizer can be excited by arbitrary linearly, circularly or elliptically polarized lights. It may generate a large localized field enhancement and maintain the polarization azimuth of linearly polarized optical field.

parallel to y -axis. Each constituent Au equilateral triangle of the bowtie has a perpendicular bisector length of 40 nm with a radius of curvature of 6.3 nm in the corner. The geometric center of bowtie nanoantenna is overlapped with those of rectangular apertures. The permittivity of gold is described by the Drude model with the relative permittivity at infinite frequency $\epsilon_\infty=9.0$, the plasma frequency $\omega_p = 1.3166 \times 10^{16} \text{ s}^{-1}$, and the damping constant $\gamma = 1.3464 \times 10^{14} \text{ s}^{-1}$ [22]. The linear nano-polarizer is placed on the glass substrate with permittivity of 2.25. The finite element method implemented in COMSOL Multiphysics was used to calculate the e-field distribution through the structures [23]. The linear nano-polarizer is illuminated by normally incident light from the asymmetric aperture side. Around the simulation domain, perfectly matched layers are placed to completely absorb the waves leaving the simulation domain in the direction of propagation. The near-field intensity is calculated by the maximum normalized e-field intensity in the gap region within the plane through the center of the bowtie nanoantenna in the z direction.

3. Comparison between bowtie nanoantenna and linear nano-polarizer

A number of recent publications have discussed the optical properties of solitary bowtie nanoantenna, which exhibits high localized field enhancement and outstanding spatial confinement of the applied electric field due to the plasmonic resonance and curvature effect of bowtie tips [24, 25]. However, the bowtie nanoantenna will selectively enhance the field projection along its own axis due to the strong resonance [26]. Thus, bowtie nanoantenna can only allow one field component along the antenna axis to present in the gap region. The normalized intensity spectra of the bowtie nanoantenna and linear nano-polarizer are shown in Fig. 2(a), where the polarization azimuth θ of incident light is 90° . The bowtie nanoantenna has a weak res-

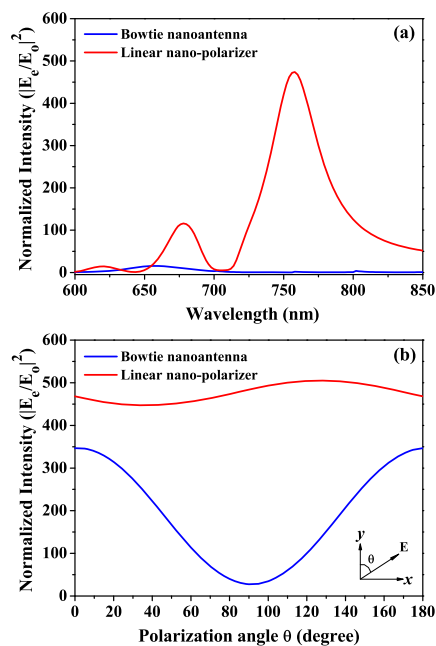


Fig. 2. (a) Comparison of normalized intensity spectra between the bowtie nanoantenna and linear nano-polarizer. The polarization azimuth θ of incident light is 90° . (b) Normalized intensity of bowtie nanoantenna and linear nano-polarizer under different incident excitation light polarizations at the resonant wavelengths of 640 nm and 760 nm, respectively.

onance. However, the proposed linear nano-polarizer has three distinct resonant peaks, which correspond to the waveguide modes of asymmetry nanoapertures. The lowest-order waveguide mode at 760 nm has the strongest resonance among three modes. Therefore, we specify this mode in the following discussions about the nano-polarizer. Figure 2(b) shows the normalized intensity of bowtie nanoantenna (blue line) and linear nano-polarizer (red line) excited by different polarizations of linearly polarized light at the resonant wavelengths of 640 nm and 760 nm, respectively. The normalized intensity of bowtie nanoantenna exhibits a strong dependence on the polarization of incident light at the resonance wavelength. When the polarization angle θ of incident light is 0° , the largest enhancement factor can be achieved. However, when the θ equals 90° , the normalized intensity is close to zero. In contrast, the normalized intensity of linear nano-polarizer shows a weak dependence on the polarization of incident light at the resonance wavelength. It can still exhibit large localized field enhancement at the polarization angle of 90° , where has not the field component of incident light along the antenna axis. In order to quantify the dependence of incident polarization to the nanostructure, the polarization feature can be characterized by the polarization contrast P as $P=(I_{max}-I_{min})/(I_{max}+I_{min})$, where I_{max} and I_{min} are the measured maximum and minimum normalized intensity under different polarizations of incident light at fixed wavelength, respectively. The polarization contrast for bowtie nanoantenna is approximately equal to 1, showing strong sensitivity to the polarization of incident light, which follows the previous result [27]. On the contrary, the polarization contrast for the linear nano-polarizer is 0.06, which shows a weak sensitivity to the polarization of incident light.

To further understand the differences of near-field distribution, we give the normalized near-field spatial distribution for solitary bowtie nanoantenna and linear nano-polarizer at the resonant wavelengths of 640 nm and 760 nm, in Figs. 3(a) and 3(b), respectively. As expected, when the polarization azimuth of incident light was perpendicular to the pair of triangles, most of the e-fields are assembled near the four endpoint of the bowtie nanoantenna, as shown in Fig. 3(a). The e-fields can not be found in the gap region of bowtie nanoantenna. However, the linear nano-polarizer can still make a large enhancement and concentrate light on nanoscale in its gap region [see in Fig. 3(b)] even though the polarization of incident light is perpendicular

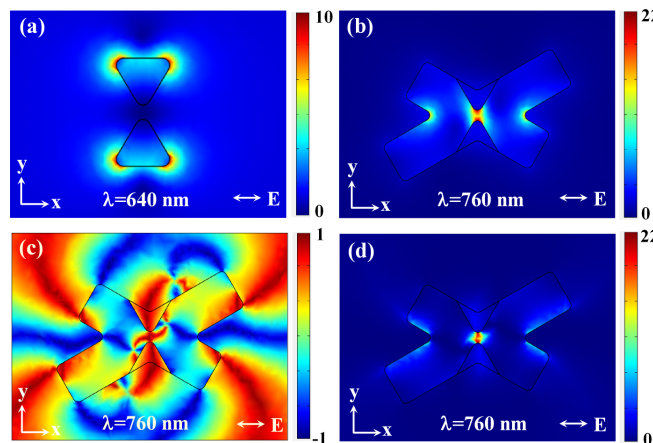


Fig. 3. Normalized near-field spatial distribution for (a) bowtie nanoantenna and (b) linear nano-polarizer with the polarization azimuth of incident light along x direction at the resonant wavelengths of 640 nm and 760 nm, respectively. Distribution of (c) parameter C and (d) modified figure of merit f for linear nano-polarizer.

to the bowtie nanoantenna axis. In order to analyze the polarization state of optical field in gap region, we consider a modified Stokes parameter $S_2 = \langle E_y(t)^2 - E_x(t)^2 \rangle$, where $\langle \bullet \rangle$ denotes time average, $E_x(t)$ and $E_y(t)$ are the electric field amplitudes [28]. We also define a degree of polarization as $C = \frac{S_2}{\langle E_x(t)^2 + E_y(t)^2 \rangle}$, for which $C = 1$ or $C = -1$ present a perfect linear polarization along the y or x axis, respectively. Spatial map of C is shown in Fig. 3(c), providing evidence that a fairly uniform and almost unitary polarization optical field ($C \approx 1$) is obtained over the area inside the gap region. Figure 3(d) shows an accordingly modified figure of merit $f = I \times \langle \frac{E_y(t)^2}{E_x(t)^2 + E_y(t)^2} \rangle$ [29], confirming that the linear nano-polarizer can not only rotate the polarization azimuth of the incident wave by 90° in the near-field, but also exhibit large localized field enhancement and outstanding spatial confinement of the translated optical field in the gap region. The discrepancy of e-field distribution between the bowtie nanoantenna and linear nano-polarizer can be attributed to the introduction of asymmetric nanoaperture. Under the illumination of the incident light polarized perpendicular to the pair of triangles, two arms of asymmetric nanoaperture can introduce a specific phase difference by adjusting the values of L_1 and L_2 , which leads to the conversion of the polarization state for the incident light. Therefore, the e-field component along the pair of bowtie nanoantenna can be generated in the process of the interaction between the asymmetric nanoaperture and incident light, which can be further concentrated by bowtie nanoantennas resulting in a large near-field enhancement in the gap region. The asymmetric nanoaperture plays an important role in controlling the polarization azimuth of the linearly polarized optical field in the near-field.

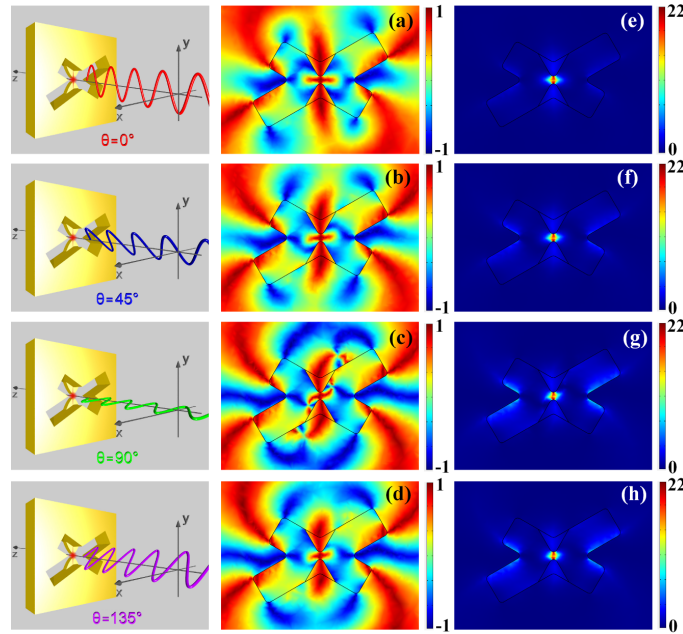


Fig. 4. Spatial distribution of parameters C ((a)-(d)) and f ((e)-(h)) for linear nano-polarizer illuminated under different polarizations of linearly incident light. The schematic configurations show four incident polarization angles of linearly polarized light are calculated.

4. Optical properties of linear nano-polarizer

In order to comprehensively demonstrate the optical property of the linear nano-polarizer, we calculated the spatial distribution of parameters C and f illuminated under different polarizations of linearly incident light in Fig. 4. The polarization angle of incident light has an interval of 45° from 0° to 135° . Although the distributions of parameter C have a slight difference from each other, a fairly uniform and almost unitary polarization optical field ($C \approx 1$) can be obtained in the gap region for four different polarization azimuths, as shown in Figs. 4(a)-4(d). Moreover, the linear nano-polarizer also exhibits large localized field enhancement and outstanding spatial confinement of linearly y -polarized optical field in the gap region for different polarizations of excitation light, which can be seen in Figs. 4(e)-4(h). Meanwhile, the normalized intensity in the gap region is almost same with each other consisting with the low polarization contrast $P=0.06$. Based on these capabilities, the linear nano-polarizer can be employed to freely control the polarization azimuth of linearly polarized optical field in the near-field through rotating the nano-structure, regardless of the polarization of excitation light. Our proposed linear nano-polarizer can not only realize the function of Glan-Taylor polarizer in the near-field making the miniaturization of linear polarizer possible, but also get rid of strong dependence on the polarization of the incident light.

As mentioned above, the weak sensitivity of linear nano-polarizer to the incident polarization can be attributed to the conversion of the polarization state for the incident light by asymmetric nanoaperture. In order to further display the influence of asymmetry nanoaperture, we simulated the spectra of polarization contrast P and minimum normalized intensity I_{min} as a function of L_1 in Figs. 5(a) and 5(b), respectively, where L_2 is fixed at 170 nm. Results show that low polarization contrast P can be obtained in a wide range (blue area in Fig. 5(a)), exhibiting a weak polarization sensitivity for the presented linear nano-polarizer. The linear nano-polarizer can

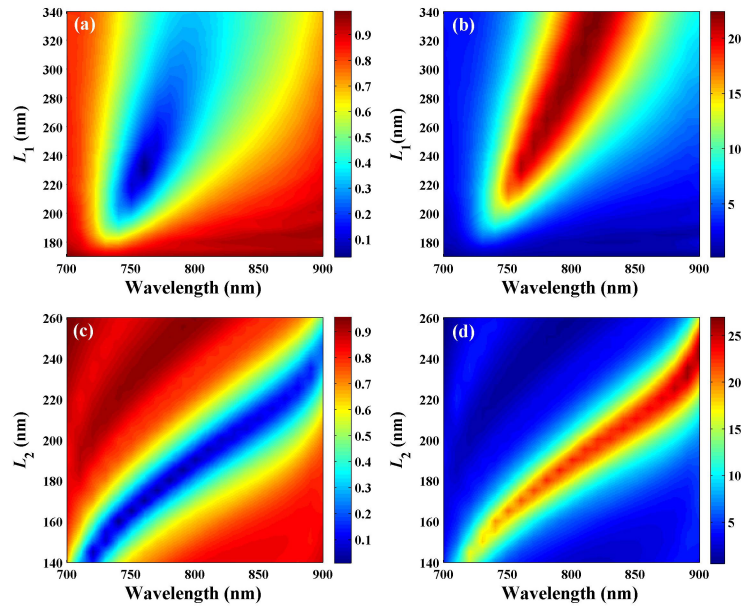


Fig. 5. Spectra of (a) polarization contrast P and (b) minimum normalized intensity I_{min} as a function of L_1 , where L_2 is fixed at 170 nm. Spectra of (c) polarization contrast P and (d) minimum normalized intensity I_{min} as a function of L_2 , where the ratio of the L_1 and L_2 is fixed at 1.35.

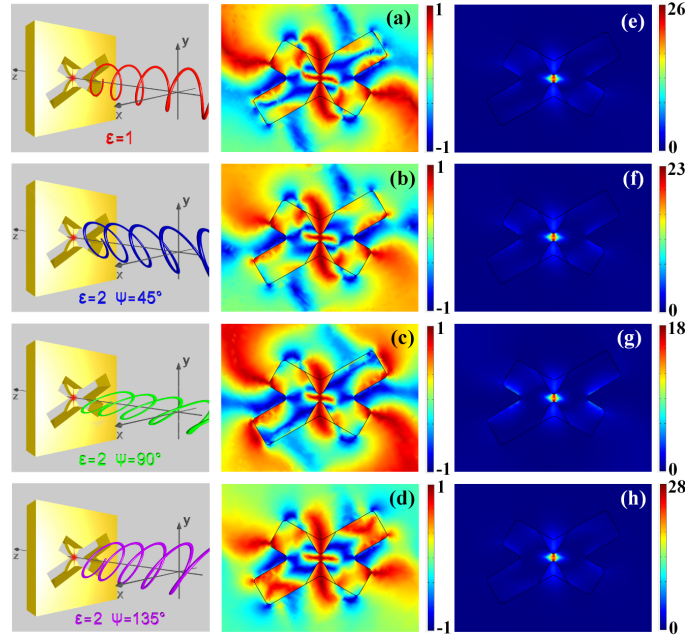


Fig. 6. Spatial distribution of C ((a)-(d)) and f ((e)-(h)) for linear nano-polarizer illuminated by circularly and elliptically polarized lights. The schematic configurations show circularly polarized light and elliptically polarized light with different azimuth angles are calculated.

also concentrate light on nanoscale in its gap region and realize a large localized field enhancement (red area in Fig. 5(b)). When the optimum ratio of the L_1 and L_2 is 1.35 with $L_1=230$ nm and $L_2=170$ nm, the minimum polarization contrast P can be obtained, corresponding to the previous geometry parameters in Fig. 2. Figures 5(c) and 5(d) show the spectra of polarization contrast P and minimum normalized intensity I_{min} as a function of L_2 , where the ratio of the L_1 and L_2 is fixed at 1.35. The wavelength corresponding to the low polarization contrast P exhibits an obvious red shift with the increasing of L_2 , meanwhile maintaining large localized field enhancement. Therefore, the near-field linear nano-polarizer can be used in a wide wavelength range through adjusting geometrical parameters, which will be highly desirable for practical applications.

In order to explore the optical response of our linear nano-polarizer to other polarization states, we calculated the spatial distribution of C and f for linear nano-polarizer illuminated by circularly and elliptically polarized lights in Fig. 6. The ellipticity ε (the major-to-minor-axis ratio) of elliptically polarized light is fixed at 2, and three azimuth angles (the angle between the major semi-axis and the x -axis) with 45° , 90° and 135° are calculated. An almost unitary polarization optical field ($C \approx 1$) and large localized enhancement can still be obtained in the gap region for circularly and elliptically polarized lights. Therefore, the linearly polarized optical field shows a weak sensitive to arbitrary linearly, circularly or elliptically polarized light.

5. Conclusion

In conclusion, we have demonstrated a linear nano-polarizer composed of asymmetric nanoaperture and bowtie nanoantenna, which provides a new way to freely control the polarization azimuth of the translated optical field in the near-field. The proposed linear nano-polarizer can not only realize the function of Glan-Taylor polarizer in the near-field, but also get rid of

strong dependence on the polarization of the incident light. The response wavelength of the linear nano-polarizer can be easily tuned in a wide range by adjusting the geometrical parameters of asymmetric nanoaperture. We believe this linear nano-polarizer enables us to modulate electromagnetic wave polarizations flexibly, and is potentially useful in applications such as polarizing plate, sensor, and integrated with other optical devices for polarization manipulation, detection, and sensing at the nanoscale.

Acknowledgments

This work was supported by the Chinese National Key Basic Research Special Fund (2011CB922003), the National Basic Research Program (973 Program) of China (2012CB921900), the Natural Science Foundation of China (61008002), the Specialized Research Fund for the Doctoral Program of Higher Education (20100031120005 and 20120031120032), the Fundamental Research Funds for the Central Universities, and the 111 project (B07013).